Instantaneous Control of Backward-Facing Step Flows

Haecheon Choi*, **Michael Hinze**† & **Karl Kunisch**&

* Dept. of Mechanical Engng, Seoul National University, Seoul 151-742, Korea
† Fachbereich Mathematik, MA 6-3, Technische Universität Berlin 10623 Berlin, Germany
& Institut für Mathematik, Universtität Graz, A-8010 Graz, Austria

Abstract

In the present paper suboptimal boundary control strategies for the time-dependent, incompressible flow over the backward-facing step are considered. The objective consists in the reduction of the recirculation bubble of the flow behind the step. Several cost functionals are suggested and a frame for the derivation of the optimality systems for a general class of cost functionals is presented. Numerical examples are given.

1 Problem formulation

The main objective of the present work is the development of a numerically realizable robust control technique in order to reduce the recirculation bubble behind the step, and thus reducing the re-attachment length of a backward-facing-step flow by controlling the flow at the boundary near the edge of the step. For the following presentation it will be convenient to refer to Fig. 1 which depicts the spatial domain Ω that constitutes the flow region and the subsets of the boundary that we shall refer to. Let (u_1, u_2, u_3) denote the velocity of the

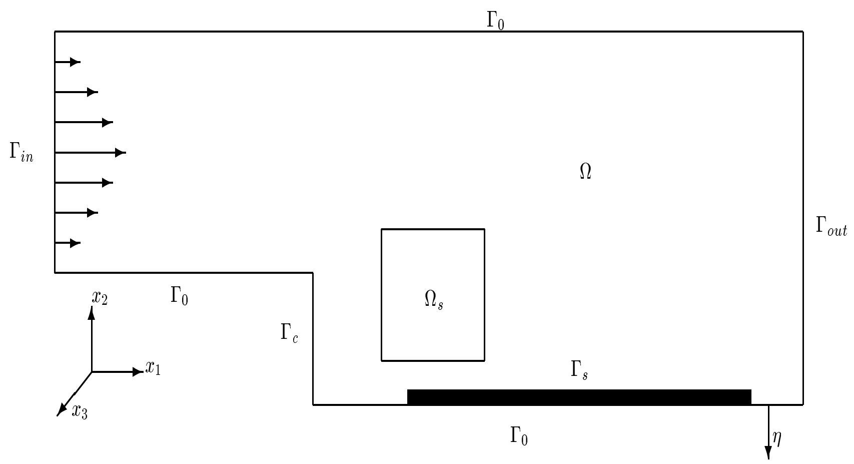

Figure 1: Flow region

fluid in the directions (x_1, x_2, x_3) and let p denote its pressure. The time-dependent Navier-Stokes equations on the space-time cylinder $Q := \Omega \times (0, T)$, $T > 0$ are given by

$$\left.\begin{array}{rcl} u_t - \frac{1}{Re}\Delta u + (u \cdot \nabla)u + \nabla p & = & f \\ -div\, u & = & 0 \end{array}\right\} \quad \text{in } Q, \tag{1}$$

where f is a prescribed volume force, Δ denotes the (3×3) matrix with Δ in its diagonal and zero otherwise, $(u \cdot \nabla)u$ stands for the vector with components $\sum_{j=1}^{3} u_j \frac{\partial}{\partial x_j} u_i$ and $Re = \frac{UH}{\nu}$ denotes the Reynolds number with U denoting the bulk velocity of the inlet profile, H the step height and ν the kinematic viscosity. Further we have chosen dimension three for presenting the theoretical part of our approach. At $t = 0$ the initial condition

$$u(x, 0) = u_0(x) \quad \text{for } x \in \Omega \tag{2}$$

is imposed, where u_0 is a given function on Ω.

Next we describe the boundary conditions. On the inflow boundary Γ_{in} we prescribe an inhomogeneous Dirichlet condition

$$u(\cdot, t) = u_{in} \quad \text{on } \Gamma_{in}, \tag{3}$$

where u_{in} is given and will be taken as a parabolic inflow profile in the numerical examples. On the outflow part of the boundary we prescribe a natural (" do-nothing") boundary condition

$$\frac{1}{Re} \partial_\eta u = p\eta \quad \text{on } \Gamma_{out}, \tag{4}$$

where η denotes the unit normal to $\partial\Omega$ in outward direction. This boundary condition is used as a downstream condition in [4] and it was observed numerically in [5], e.g. that this choice of boundary condition has little artificial influence on practically observed flow patterns. On the remaining part of the boundary, except for the control portion Γ_c, no-slip boundary conditions are assumed:

$$u = 0 \quad \text{on } \partial\Omega \setminus (\Gamma_{in} \cup \Gamma_{out} \cup \Gamma_c). \tag{5}$$

Finally, in order to influence the flow in the recirculation zone behind the step a control will be applied along the boundary Γ_c,

$$u = \phi \quad \text{on } \Gamma_c. \tag{6}$$

Here ϕ denotes the control function representing blowing and suction which will be chosen in such a manner that an appropriately defined performance index is minimized. It will be convenient to combine the Dirichlet boundary conditions (3) and (5) into one statement

$$u = g \quad \text{on } \Gamma_d := \partial\Omega \setminus (\Gamma_{out} \cup \Gamma_c), \tag{7}$$

where $g = u_{in}$ on Γ_{in} and zero otherwise.

The choice of the cost functional appropriate to capture the goal of influencing and reducing the recirculation bubble is certainly a delicate one. Here we shall primarily consider functionals of the form

$$J(\phi) = \int_0^T \left[\int_{\Gamma_s} F(\partial_\eta u)\, d\Gamma_s \; + \; \frac{\gamma}{2} \int_{\Gamma_c} \phi^2 \, d\Gamma_c \right] dt, \tag{8}$$

where $\gamma > 0$ and $F : \mathbb{R}^3 \to \mathbb{R}$ is a given, sufficiently smooth function. Referring to Fig. 1 we have $\eta = (0, -1, 0)^t$ on Γ_s and hence a special case of (8) is given by

$$J(\phi) = \int_0^T \left[\int_{\Gamma_s} \frac{1}{2} \frac{\partial u_1}{\partial x_2} \left(\frac{\partial u_1}{\partial x_2} - \left| \frac{\partial u_1}{\partial x_2} \right| \right) d\Gamma_s \; + \; \frac{\gamma}{2} \int_{\Gamma_c} \phi^2 \, d\Gamma_c \right] dt. \tag{9}$$

The first part of the cost penalizes a negative wall velocity gradient in the sensor area Γ_s which is supposed to contain the re-attachment point. The second summand weights the costs for the control acting along Γ_c.

Other functionals involving shear stresses or drag along Γ_s can be expressed as special cases of (8). We can now state the optimal control problem which is the focus of this paper.

$$(P)\quad \begin{cases} \min J(\phi) = \int_0^T \left[\int_{\Gamma_s} F(\partial_\eta u)\, d\Gamma_s \;+\; \frac{\gamma}{2}\int_{\Gamma_c} \phi^2\, d\Gamma_c\right] dt \\ \text{s.t.} \\ \begin{aligned} u_t - \tfrac{1}{Re}\Delta u + (u\cdot\nabla)u + \nabla p &= f && \text{in } Q \\ -div\, u &= 0 && \text{in } Q \\ u &= g && \text{on } \Gamma_d \times (0,T] \\ u &= \phi && \text{on } \Gamma_c \times (0,T] \\ \tfrac{1}{Re}\partial_\eta u &= p\eta && \text{on } \Gamma_{out} \times (0,T] \\ u(0) &= u_0 \end{aligned} \end{cases} \tag{10}$$

Before closing this section let us make some comments on alternative choices of cost functionals. For this purpose let $\Omega_s \subset \Omega$ denote an observation volume inside Ω. We carried out several numerical experiments for the cost functional

$$J_1(\phi) = \frac{1}{2}\int_0^T \left[\int_{\Omega_s} |u - u_{st}|^2\, dx \;+\; \gamma\int_{\Gamma_c} \phi^2\, d\Gamma_c\right] dt, \tag{11}$$

where u_{st} denotes the Stokes flow in Ω. The discussions of Sections 2 and 3 can easily be adapted to this cost functional involving tracking to the laminar Stokes flow.

Important experimental work on the reduction of the separation bubble is related to the enhancement of mixing right after the edge of the step. The cost functional (9) does not take this into account. A proper cost functional to be minimized would be given by

$$J_2(\phi) = \int_0^T \left[\int_{\Omega_s} \frac{1}{1+\frac{1}{2}({u'_1}^2 + {u'_2}^2 + {u'_3}^2)}\, dx \;+\; \frac{\gamma}{2}\int_{\Gamma_c} \phi^2\, d\Gamma_c\right] dt$$

which corresponds to the increase of the turbulent kinetic energy in Ω_s, where Ω_s would be taken as an observation volume right behind the tip of the step. Here u'_i denotes the fluctuation with respect to the mean value of the uncontrolled flow. An interesting choice of cost functional describes the enhancement of the streamwise vorticity near the edge of the step:

$$J_3(\phi) = \int_0^T \left[\int_{\Omega_s} \frac{1}{1+\omega_1^2}\, dx \;+\; \frac{\gamma}{2}\int_{\Gamma_c} \phi^2\, d\Gamma_c\right] dt,$$

where $\omega_1 = \frac{\partial u_3}{\partial x_2} - \frac{\partial u_2}{\partial x_3}$. Note that $\omega_1 = 0$ in two dimensional flows and thus this definition of cost is only meaningful in three dimensional calculations. The evaluation of the costs J_1, J_2 and J_3 requires information of the velocity or its derivatives inside the flow region. These quantities are also necessary to compute the adjoint equations. This may limit the applicability of these types of cost functionals for feedback control since information on the velocities in Ω is difficult to obtain. As we shall see below, these quantities appear in the right-hand side of the adjoint equations. However, results based on these types of cost functionals are valuable for comparisons with cost $J(\phi)$.

The enhancement of the streamwise vortices on the tip of the step may be a good choice as well. In this case the cost becomes

$$J_4(\phi) = \int_0^T \left[\int_{\Gamma_T} \frac{1}{1+\omega_1^2}\, d\Gamma_T \;+\; \frac{\gamma}{2}\int_{\Gamma_c} \phi^2\, d\Gamma_c\right] dt,$$

where Γ_T denotes an area on the tip. Since $|\frac{\partial u_3}{\partial_{x_2}}| >> |\frac{\partial u_2}{\partial_{x_3}}|$ in most wall bounded flows, one could assume $\omega_1 \approx \frac{\partial u_3}{\partial_{x_2}}$. With Γ_s replaced by Γ_T this results in a special case of J according to (8).

Let us briefly outline the contents of the following sections. In Section 2 we present the optimality system for problem (P). It will be seen that its numerical realization is beyond todays workstation capabilities. Hence, following Choi, Temam, Moin and Kim [3] we develop in Section 3 a suboptimal control strategy amenable for workstation implementation. It will also be shown that a near to optimal line search rule can be implemented in the gradient algorithm at the expense of two additional quasi-Stokes solutions at each iteration level only. Numerical results will be given in Section 4.

2 The optimality system for (P)

This section is devoted to the formal derivation of the optimality system related to problem (10) based on a Lagrangian approach. Further the gradient $\nabla J(\phi)\chi$ of J at ϕ in direction χ will be characterized. For a similar derivation see also Abergel and Temam [1].

Henceforth, let ϕ^* denote a solution to (10) and let $(u^*, p^*) = (u(\phi^*), p(\phi^*))$ denote the corresponding optimal velocity field and pressure, respectively satisfying the Navier-Stokes system. Then (u^*, p^*, ϕ^*) satisfies the following system of coupled equations in the 'primal variables' (u, p, ϕ) and the 'adjoint variables' (ξ, π, μ):

$$\begin{array}{rcl}
u_t - \frac{1}{Re}\Delta u + (u\cdot\nabla)u + \nabla p &=& f \quad \text{in } Q \\
-div\, u &=& 0 \quad \text{in } Q \\
u &=& \left\{\begin{array}{ll} g & \text{on } \Gamma_d \times (0,T] \\ \phi & \text{on } \Gamma_c \times (0,T] \end{array}\right. \\
\frac{1}{Re}\partial_\eta u &=& p\eta \quad \text{on } \Gamma_{out} \times (0,T] \\
u(0) &=& u_0 \\
-\xi_t - \frac{1}{Re}\Delta\xi + (\nabla u)^t\xi - (u\cdot\nabla)\xi + \nabla\pi &=& 0 \quad \text{in } Q \\
-div\, \xi &=& 0 \quad \text{in } Q \\
\xi &=& \left\{\begin{array}{ll} 0 & \text{on } \partial\Omega \setminus (\Gamma_{out}\cup\Gamma_s) \times (0,T] \\ Re\nabla F(\partial_\eta u) & \text{on } \Gamma_s \times (0,T] \end{array}\right. \\
\xi(T) &=& 0 \\
\frac{1}{Re}\partial_\eta\xi + (u\cdot\eta)\xi &=& \pi\eta \quad \text{on } \Gamma_{out} \times (0,T] \\
\gamma\phi + \frac{1}{Re}\partial_\eta\xi &=& \pi\eta \quad \text{on } \Gamma_c \times (0,T].
\end{array} \tag{12}$$

Here $((\nabla u)^t\xi)_i = \sum_j(\partial_{x_i}u_j)\xi_j$. The gradient of J at ϕ in direction χ is given by

$$\nabla J(\phi)\chi = \int_0^T \int_{\Gamma_c} (\gamma\phi + \frac{1}{Re}\partial_\eta\xi - \pi\eta)\,\chi\, d\Gamma_c dt, \tag{13}$$

where (ξ, π) are computed from (12) with (u^*, p^*, ϕ^*) replaced by (u, p, ϕ). We observe that the primal and dual variables are strongly coupled in system (12). The coupling in the coefficient of the state equation for ξ and the boundary condition on Γ_{out} for ξ is due to the nonlinear character of the Navier-Stokes equations. The coupling between ϕ and (ξ, π) and the fact that the primal equation is solved forward whereas the adjoint equation for (ξ, π) is solved backwards in time are characteristic for optimal control problems. Since solving (12) numerically is beyond the todays workstation capabilities, suboptimal control strategies that can be realized numerically will be developed in the following sections.

For the special case of J given in (9) and the geometry of Fig. 1 we have (note that $\eta = (0,-1,0)^t$)

$$F(z_1, z_2, z_3) = \frac{1}{2} z_1 (z_1 + |z_1|)$$

and

$$\nabla F(\partial_\eta u) = \begin{pmatrix} -\frac{\partial u_1}{\partial x_2} + \left|\frac{\partial u_1}{\partial x_2}\right| \\ 0 \\ 0 \end{pmatrix}$$

As a guideline for the following formal derivation it will be useful to recall that the gradient of J at ϕ in direction χ for the following equality constrained optimal control problem

$$\begin{cases} \min J(\phi) = F(y) + \frac{\gamma}{2}|\phi|^2 \\ \text{s.t.} \\ e(y,\phi) = 0 \end{cases} \tag{14}$$

with state variable u and control variable ϕ is given by

$$J'(\phi)\chi = (e_\phi^* \lambda + \gamma\phi, \chi), \tag{15}$$

where λ satisfies the adjoint equation

$$e_y^* \lambda = -F'(y). \tag{16}$$

The inner product in (15) is the one of the control space and e_ϕ^* denotes the transpose of e_ϕ. Further e_ϕ stands for the linearization of e w.r.t. ϕ. Similarly $F'(y)$ denotes the linearization of F at y and e_y^* is the transpose of the linearization of e w.r.t. y.

The Lagrangian related to (14) is given by

$$L(y,\phi,\lambda) = F(y) + \frac{\gamma}{2}|\phi|^2 + \langle \lambda, e(y,\phi)\rangle,$$

with $< \cdot, \cdot >$ the inner product of the range space of e.

Let us note that $L_y = 0$ is equivalent to

$$L_y = e_y^* \lambda + F'(y) = 0, \tag{17}$$

which is (16), and further

$$L_\phi(\phi)\chi = (e_\phi^* \lambda + \gamma\phi, \chi)$$

so that by (15)

$$L_\phi(\phi)\chi = \nabla J(\phi)\chi. \tag{18}$$

We associate to (10) the Lagrangian

$$\begin{aligned} L(u,p,\phi,\xi,\pi,\mu) \quad = \quad & \int_0^T \left[\int_{\Gamma_s} F(\partial_\eta u)\, d\Gamma_s \ dt + \frac{\gamma}{2} \int_{\Gamma_c} \phi^2 \, d\Gamma_c \right] dt \\ & + \int_0^T \int_\Omega (u_t - \frac{1}{Re}\Delta u + (u\cdot\nabla)u + \nabla p)\xi \, dx dt - \int_0^T \int_\Omega \pi \, div\, u \, dx dt + \int_0^T \int_{\Gamma_c} (u-\phi)\mu \, d\Gamma_c dt. \end{aligned}$$

Here

$$u(\cdot,0) = u_0 \text{ in } \Omega, \ \ u = g \text{ on } \Gamma_d \times (0,T] \text{ and } \frac{1}{Re}\partial_\eta u = p\eta \text{ on } \Gamma_{out} \times (0,T] \tag{19}$$

are kept as explicit constraints. The partial derivatives of L w.r.t. u, p and ϕ in direction w, q and χ are given by

$$
\begin{aligned}
L_u(w) &= \int_0^T \int_{\Gamma_s} \nabla F(\partial_\eta u)\, \partial_\eta w \, d\Gamma_s dt + \int_0^T \int_\Omega (w_t - \frac{1}{Re}\Delta w + (u\cdot\nabla)w + (w\cdot\nabla)u)\xi - \pi div\, w \; dxdt \\
&\quad + \int_0^T \int_{\Gamma_c} w\mu \, d\Gamma_c dt, \qquad (20)\\
L_p(q) &= \int_0^T \int_\Omega \xi \nabla q \, dxdt, \qquad (21)\\
L_\phi(\chi) &= \int_0^T \int_{\Gamma_c} (\gamma\phi - \mu)\chi \, d\Gamma_c dt, \qquad (22)
\end{aligned}
$$

where the derivatives are taken at (ξ, π, μ). Equation (17) thus becomes

$$L_u(w) + L_p(q) = 0 \qquad (23)$$

for all (w, q) satisfying

$$w(\cdot, 0) = 0 \text{ in } \Omega,\; w = 0 \text{ on } \Gamma_d \times (0, T] \text{ and } \frac{1}{Re}\partial_\eta w = q\eta \text{ on } \Gamma_{out} \times (0, T]. \qquad (24)$$

Next let us derive the properties for (ξ, π, μ) resulting from (23). By (21) and (23) with $w = 0$ and q having compact support in Q we obtain

$$div\, \xi = 0 \quad \text{in } Q, \qquad (25)$$

and with q having arbitrary values on $(\partial\Omega \setminus \Gamma_{out}) \times (0, T]$ it follows that

$$\xi\eta = 0 \quad \text{on } (\partial\Omega \setminus \Gamma_{out}) \times (0, T]. \qquad (26)$$

Choosing w with compact support in Q and $q = 0$, (20) and (23) imply

$$-\xi_t - \frac{1}{Re}\Delta\xi + (\nabla u)^t \xi - (u\cdot\nabla)\xi + \nabla\pi = 0 \quad \text{in } Q. \qquad (27)$$

From (20) and (23) it further follows that

$$\xi(\cdot, T) = 0 \quad \text{in } \Omega. \qquad (28)$$

Let us now turn to the properties resulting from (23) for the boundary conditions of ξ. From (23)-(28) it follows for test functions satisfying $w = 0$ on $\Gamma_{out} \cup \Gamma_d$, $q = 0$ that

$$\int_{\Gamma_s} \nabla F(\partial_\eta u)\partial_\eta w \, d\Gamma_s - \frac{1}{Re}\int_{\partial\Omega} \partial_\eta w \xi \, d\Gamma + \int_{\Gamma_c} (\frac{1}{Re} w \partial_\eta \xi + (u\cdot\eta)\xi w - \pi w\cdot\eta + w\mu)\, d\Gamma_c = 0 \qquad (29)$$

almost everywhere in $(0, T)$. If further $w = 0$ on all of $\partial\Omega$ and $\partial_\eta w = 0$ on $\Gamma_{out} \cup \Gamma_s$ then

$$\int_{\partial\Omega\setminus(\Gamma_{out}\cup\Gamma_s)} \partial_\eta w\xi \, d\Gamma = 0$$

and hence

$$\xi = 0 \quad \text{on } (\partial\Omega \setminus (\Gamma_{out} \cup \Gamma_s)) \times (0, T] = ((\Gamma_d \setminus \Gamma_s) \cup \Gamma_c) \times (0, T]. \qquad (30)$$

For test functions w that are arbitrary on Γ_c and satisfy $w = 0$ on $\Gamma_d \cup \Gamma_{out}$ as well as $\partial_\eta w = 0$ on $\Gamma_s \cup \Gamma_{out}$ we derive from (29) and (30)

$$\frac{1}{Re}\partial_\eta \xi + \mu = \pi\eta \quad \text{on } \Gamma_c. \tag{31}$$

Utilizing (23) a third time with $\partial_\eta w$ arbitrary on Γ_s and 0 on $\partial\Omega \setminus \Gamma_s$. Equations (29) and (31) yield

$$Re\, \nabla F(\partial_\eta u) = \xi \quad \text{on } \Gamma_s \times (0, T]. \tag{32}$$

In order to derive a boundary condition for (ξ, π) on Γ_{out} we utilize (23) with (w, q) satisfying (24) and w as well as $\partial_\eta w$ equal to 0 on $(\partial\Omega \setminus \Gamma_{out}) \times (0, T]$. A short calculation using (26) implies

$$\frac{1}{Re}\partial_\eta \xi + (u \cdot \eta)\xi = \pi\eta \quad \text{on } \Gamma_{out}. \tag{33}$$

Let us summarize the computations so far. From (25)-(28) we obtain the adjoint equation in the variables (ξ, π, μ)

$$\begin{aligned}
-\xi_t - \tfrac{1}{Re}\Delta\xi + (\nabla u)^t\xi - (u\cdot\nabla)\xi + \nabla\pi &= 0 \quad \text{in } Q \\
-div\,\xi &= 0 \quad \text{in } Q \\
\xi &= \begin{cases} 0 & \text{on } (\partial\Omega \setminus (\Gamma_{out} \cup \Gamma_s)) \times (0,T] \\ Re\nabla F(\partial_\eta u) & \text{on } \Gamma_s \times (0,T] \end{cases} \\
\tfrac{1}{Re}\partial_\eta\xi + (u\cdot\eta)\xi &= \pi\eta \quad \text{on } \Gamma_{out} \times (0,T] \\
\xi(T) &= 0 \\
\tfrac{1}{Re}\partial_\eta\xi + \mu &= \pi\eta \quad \text{on } \Gamma_c \times (0,T] \\
\xi\eta &= 0 \quad \text{on } \Gamma_s \times (0,T].
\end{aligned} \tag{34}$$

Next we briefly discuss the above system of equations. The first five equations in (34) are the adjoint system for (P) (see (12)). Utilizing the fourth equality in (34) the last equation can equivalently be expressed as

$$\nabla F(\partial_\eta u) \cdot \eta = 0 \quad \text{on } \Gamma_s \times (0, T]. \tag{35}$$

This can be considered as a compatibility condition for F (or u). It is trivially satisfied for the choice of F in (9). The next to last condition in (34) allows a simple presentation of the gradient of J w.r.t. ϕ. In fact, utilizing (23) and (22) we get

$$\nabla J(\phi)\chi = L_\phi(\chi) = \int_0^T \int_{\Gamma_c} (\gamma\phi + \frac{1}{Re}\partial_\eta\xi - \pi\eta)\,\chi\, d\Gamma_c dt,$$

as claimed in (13). The optimality condition $\nabla J(\phi) = 0$ can be expressed as

$$\gamma\phi + \frac{1}{Re}\partial_\eta\xi = \pi\eta,$$

which coincides with the last equation in (12) and concludes the formal derivation of the optimality system for (10).

3 The instantaneous control strategy

As pointed out in the previous section solving the optimality system (12) is almost unworkable at this time. This suggests the use of suboptimal control strategies. A second motivation for such strategies is given by closed-loop control considerations as will shortly be explained.

The approach that we take is based on a time discretization of (10). At each discrete time level t_i a stationary control problem is solved for an optimal control ϕ_i^* and this control is used to steer the system from t_i to t_{i+1}, where a new optimal control is determined. It cannot be claimed that the controls obtained in this manner approximate the optimal control for (10) as the discretization parameter tends to zero. However, this procedure will be justified by the effectiveness that it exhibits for numerical examples and the interpretation that it allows for suboptimal feedback controls.

To commence, let $m > 1$ be fixed and set $\delta t = \frac{T}{m}$, $t_i = i\delta t, i = 0, \ldots, m$. As an intermediate step in the derivation let us consider the case where the Navier-Stokes equations in (12) are approximated by a Crank-Nicolson scheme. At the i-th level of the Crank-Nicolson based suboptimal strategy one solves the following stationary optimal control problem (compare also [3]), where the variables (u, p, ϕ) correspond to $(u(t_i), p(t_i), \phi(t_i))$.

$$\left.\begin{array}{l} \min J(\phi) = \int_{\Gamma_s} F(\partial_\eta u)\, d\Gamma_s + \frac{\gamma}{2}\int_{\Gamma_c} \phi^2\, d\Gamma_c \\ \text{s.t.} \\ \begin{array}{rcll} \frac{1}{\delta t} u + \frac{1}{2}(u\cdot\nabla)u - \frac{1}{2Re}\Delta u + \nabla p &=& R & \text{in } \Omega \\ -div\, u &=& 0 & \text{in } \Omega \\ u &=& g & \text{on } \Gamma_d \\ \frac{1}{2Re}\partial_\eta u - p\eta &=& -\frac{1}{2Re}\partial_\eta u(t_{i-1}) & \text{on } \Gamma_{out} \\ u &=& \phi & \text{on } \Gamma_c. \end{array} \end{array}\right\} \tag{36}$$

Here $R = \frac{1}{\delta t}u(t_{i-1}) + \frac{1}{2Re}\Delta u(t_{i-1}) - \frac{1}{2}(u(t_{i-1})\cdot\nabla)u(t_{i-1}) + f(t_{i-\frac{1}{2}})$ is a known inhomogeneity. Let $\phi_i = \phi(t_i)$ denote a solution to (36) and set $(u_i, p_i) = (u(\phi_i), p(\phi_i))$. Then the triple (u_i, p_i, ϕ_i) satisfies the optimality system for (36) given by the equality constraints in (36), together with the adjoint equation

$$\left.\begin{array}{rcll} \frac{1}{\delta t}\xi_i - \frac{1}{2}(u_i\cdot\nabla)\xi_i + \frac{1}{2}(\nabla u_i)^t\xi_i &=& \frac{1}{2Re}\Delta\xi_i - \nabla\pi_i & \text{in } \Omega \\ -div\,\xi_i &=& 0 & \text{in } \Omega \\ \xi_i &=& \left\{\begin{array}{ll} 0 & \text{on } \partial\Omega\setminus(\Gamma_{out}\cup\Gamma_s) \\ 2Re\nabla F(\partial_\eta u_i) & \text{on } \Gamma_s \end{array}\right. & \\ \frac{1}{2Re}\partial_\eta\xi_i + \frac{1}{2}(u_i\cdot\eta)\xi_i &=& \pi_i\eta & \text{on } \Gamma_{out} \end{array}\right\} \tag{37}$$

and the optimality condition

$$\gamma\phi_i + \frac{1}{2Re}\partial_\eta\xi_i = \pi_i\eta \quad \text{on } \Gamma_c, \tag{38}$$

where $(\xi_i, \pi_i) = (\xi(\phi), \pi(\phi))$. This system can be derived with the techniques developed in Section 2. Note that (37) requires information of the velocity inside the domain as well as on its boundary. For computations this requires recalculation of the system matrix for the adjoint equation whenever the primal velocity field u_i changes. Let us also note that from the feedback-control point of view, one aims for replacing u_i by observations of the system and computing ϕ_i from (37) and (38). This would require knowledge of the velocity field u_i inside Ω which is impractical. We therefore simplify further the discretization by replacing the implicit Crank-Nicolson scheme for the nonlinear equation by a semi-implicit time discretization scheme (see also Choi, Temam, Moin and Kim [3]). As discretization method we choose the implicit Euler method in the viscous term and the explicit Euler method in the nonlinear convective term. In this case only measurements of the wall shear stress will be necessary to compute the adjoint variables of the corresponding adjoint system. More precisely, let us consider the minimization problem

$$(P_i)\left\{\begin{array}{rcll} \multicolumn{4}{l}{\min J(\phi) = \int_{\Gamma_s} F(\partial_\eta u)\, d\Gamma_s + \frac{\gamma}{2}\int_{\Gamma_c} \phi^2\, d\Gamma_c} \\ \multicolumn{4}{l}{\text{s.t.}} \\ u - c\Delta u + \delta t \nabla p &=& R & \text{in } \Omega \\ -div\, u &=& 0 & \text{in } \Omega \\ u &=& g & \text{on } \Gamma_d \\ c\partial_\eta u &=& \delta t\, p\eta & \text{on } \Gamma_{out} \\ u &=& \phi & \text{on } \Gamma_c, \end{array}\right. \tag{39}$$

where $c = \frac{\delta t}{Re}$ and $R = u_{i-1} - \delta t(u_{i-1}\cdot\nabla)u_{i-1} + f_i$. Note that the information from time level t_{i-1} to t_i is passed solely through the inhomogeneity R. Let ϕ_i denote a solution to (P_i) and set again $(u_i, p_i) = (u(\phi_i), p(\phi_i))$. Minor modifications of the calculations in Section 2 show that (u_i, p_i, ϕ_i) must satisfy an optimality system consisting of the primal equations which are the equality constraints in (39) and an adjoint equation, coupled with an optimality condition which are given next:

$$\left.\begin{array}{rcll} \xi_i - c\Delta\xi_i + \nabla\pi_i &=& 0 & \text{in } \Omega \\ -\delta t\, div\, \xi_i &=& 0 & \text{in } \Omega \\ \xi_i &=& \left\{\begin{array}{ll} 0 & \text{on } \partial\Omega \setminus (\Gamma_{out}\cup\Gamma_s) \\ \frac{1}{c}\nabla F(\partial_\eta u_i) & \text{on } \Gamma_s \end{array}\right. & \\ c\partial_\eta \xi_i &=& \pi_i \eta & \text{on } \Gamma_{out} \end{array}\right\} \tag{40}$$

$$\gamma\phi_i + c\partial_\eta\xi_i = \pi_i\eta \quad \text{on } \Gamma_c. \tag{41}$$

In the optimality system for (P_i) the coupling between primal and adjoint equations for the problems (P_i) occurs only along the observation boundary Γ_s.

The optimal control problem (10) has thus been replaced by a sequence of stationary problems (P_i) which can be realized on workstations. Moreover, if one interprets (41) as a feedback control law, then only observations of the state along the boundary Γ_s are required. To solve (39) numerically several different approaches are possible. Putting speed above accuracy a gradient algorithm with (almost) optimal step size is proposed to solve (P_i).

4 Gradient algorithm and line search

Throughout this section we concentrate on solving (39) for a fixed time level t_i. With the techniques of Section 2 (compare (13)) the gradient of J at ϕ_i is found to be

$$\nabla J(\phi_i) = (\gamma\phi_i + c\partial_\eta\xi_i - \pi_i\eta)_{|\Gamma_c}, \tag{42}$$

where (ξ_i, π_i) is a solution to (40) with (u_i, p_i) a solution of the primal equations in (P_i).

With the gradient of J available the following gradient algorithm can be used to reduce the value of the cost J in (P_i) (the subscript i is omitted):

Gradient Algorithm

1. Set $k = 0$ and choose ϕ_0,

2. Compute

$$\rho^* = \arg\min_{\rho>0} H(\rho) := J(\phi^k - \rho\nabla J(\phi^k))$$

3. Set
$$\phi^{k+1} = \phi^k - \rho^* \nabla J(\phi^k)$$

4. Set $k = k+1$ and goto 2.

In this algorithm the expensive part is step 2. We shall show next how to obtain a good approximation to ρ^* that requires only an additional solution of a primal-adjoint system. The optimal step size in the minimization problem of step 2. can be characterized via a Lagrange approach similar to the one of Section 2. Set $s := \nabla J(\phi^k)$ and consider

$$(L) \left\{ \begin{array}{l} \min H(\rho) = \int_{\Gamma_s} F(\partial_\eta u)\, d\Gamma_s + \frac{\gamma}{2} \int_{\Gamma_c} (\phi^k - \rho s)^2\, d\Gamma_c \\ \text{s.t. } u = u(\rho) \text{ a solution to} \\ \begin{array}{rcll} u - c\Delta u + \delta t \nabla p &=& R & \text{in } \Omega \\ -div\, u &=& 0 & \text{in } \Omega \\ u &=& g & \text{on } \Gamma_d \\ u &=& \phi^k - \rho s & \text{on } \Gamma_c \\ c\partial_\eta u &=& \delta t\, p\eta & \text{on } \Gamma_{out}. \end{array} \end{array} \right. \tag{43}$$

The corresponding Lagrangian is given by

$$\begin{aligned} G(u,p,\rho,\xi,\pi,\mu) = \int_{\Gamma_s} F(\partial_\eta u)\, d\Gamma_s \quad &+ \quad \frac{\gamma}{2} \int_{\Gamma_c} (\phi^k - \rho s)^2\, d\Gamma_c + \int_{\Gamma_c} (u - \phi^k + \rho s)\mu\, d\Gamma_c \\ &+ \quad \int_\Omega [(u - c\Delta u + \delta t \nabla p - R)\xi - \pi div u]\, d\Omega. \end{aligned}$$

The constraints on Γ_d and Γ_{out} are understood as explicit constraints.

A first order optimality system for (L) is given by

$$G_u(w) + G_p(q) = 0, \text{ and } \quad G_\rho = 0 \tag{44}$$

for all (w,q) satisfying $w = 0$ on Γ_d and $\frac{1}{Re}\partial_\eta w = q\eta$ on Γ_{out}. Condition (44) is equivalent to

$$\int_{\Gamma_s} \nabla F(\partial_\eta u)\partial_\eta w\, d\Gamma_s + \int_\Omega (w - c\Delta w)\xi\, dx + \delta t \int_\Omega \xi \nabla q\, dx - \int_\Omega \pi div w\, dx + \int_{\Gamma_c} w\mu\, d\Gamma_c = 0 \tag{45}$$

and

$$\int_{\Gamma_c} [\gamma(\rho s - \phi^k) + \mu] s\, d\Gamma_c = 0. \tag{46}$$

From (45) it follows that

$$\left. \begin{array}{rcl} \xi - c\Delta\xi + \nabla\pi &=& 0 \quad \text{in } \Omega \\ -\delta t div\, \xi &=& 0 \quad \text{in } \Omega \\ \xi &=& \left\{ \begin{array}{ll} 0 & \text{on } \partial\Omega \setminus (\Gamma_{out} \cup \Gamma_s) \\ \frac{1}{c}\nabla F(\partial_\eta u) & \text{on } \Gamma_s \end{array} \right. \\ c\partial_\eta \xi &=& \pi\eta \quad \text{on } \Gamma_{out}, \end{array} \right\} \tag{47}$$

and

$$c\partial_\eta \xi + \mu = \pi\eta \quad \text{on } \Gamma_c. \tag{48}$$

From (46) we have

$$\rho^* = \frac{1}{\gamma |s|^2_{L^2(\Gamma_c)}} \int_{\Gamma_c} (\gamma\phi^k - \mu) s\, d\Gamma_c$$

and hence

$$\rho^* = \frac{1}{\gamma|s|^2_{L^2(\Gamma_c)}} \int_{\Gamma_c} (\gamma\phi^k + c\partial_\eta \xi - \pi\eta) s \, d\Gamma_c \tag{49}$$

where (ξ, π) is given in (48) with (u, p) from (L). Since (u, p) and consequently (ξ, π) depend on ρ, (49) is a nonlinear equation for ρ. We shall next derive an approximation to ρ^* based on a linearization of ∇F at $\partial_\eta u(\phi)$. To begin with note first that the solution $(u, p) = (u(\rho), p(\rho))$ of the equality constraints in (L) is linear w.r.t. the inhomogeneity in the boundary condition on Γ_c and hence

$$u(\rho) = u(\phi^k) - \rho u(s), \quad p(\rho) = p(\phi^k) - \rho p(s),$$

where $(u(\phi^k), p(\phi^k))$ and $(u(s), p(s))$ are the solutions of

$$\left.\begin{array}{rcl} u(\phi^k) - c\Delta u(\phi^k) + \delta t \nabla p(\phi^k) & = & R \quad \text{in } \Omega \\ -div\, u(\phi^k) & = & 0 \quad \text{in } \Omega \\ u(\phi^k) & = & \left\{ \begin{array}{l} g \quad \text{on } \Gamma_d \\ \phi^k \text{ on } \Gamma_c \end{array} \right. \\ c\partial_\eta u(\phi^k) & = & \delta t \, p(\phi^k)\eta \quad \text{on } \Gamma_{out} \end{array} \right\} \tag{50}$$

and

$$\left.\begin{array}{rcl} u(s) - c\Delta u(s) + \delta t \nabla p(s) & = & 0 \quad \text{in } \Omega \\ -div\, u(s) & = & 0 \quad \text{in } \Omega \\ u(s) & = & \left\{ \begin{array}{l} 0 \text{ on } \Gamma_d \\ s \text{ on } \Gamma_c \end{array} \right. \\ c\partial_\eta u(s) & = & \delta t \, p(s)\eta \quad \text{on } \Gamma_{out}. \end{array} \right\} \tag{51}$$

The boundary condition for the adjoint variable along Γ_s is linearized according to

$$\nabla F(\partial_\eta(u(\phi^k) - \rho u(s))) \approx \nabla F(\partial_\eta u(\phi^k)) - \rho \nabla^2 F(\partial_\eta u(\phi^k))\partial_\eta u(s), \tag{52}$$

where $\nabla^2 F$ is the Hessian of $F : \mathbb{R}^3 \to \mathbb{R}$. Accordingly the adjoint variables are approximated by

$$\xi(\rho) \approx \xi(\phi^k) - \rho\xi(s), \quad \pi(\rho) \approx \pi(\phi^k) - \rho\pi(s),$$

where $(\xi(\phi^k), \pi(\phi^k))$ and $(\xi(s), \pi(s))$ are the solutions to

$$\left.\begin{array}{rcl} \xi(\phi^k) - c\Delta\xi(\phi^k) + \nabla\pi(\phi^k) & = & 0 \quad \text{in } \Omega \\ -\delta t div\, \xi(\phi^k) & = & 0 \quad \text{in } \Omega \\ \xi(\phi^k) & = & \left\{ \begin{array}{ll} 0 & \text{on } \Gamma_d \\ \frac{1}{c}\nabla F(\partial_\eta u(\phi^k)) & \text{on } \Gamma_s \end{array} \right. \\ c\partial_\eta \xi(\phi^k) & = & \pi(\phi^k)\eta \quad \text{on } \Gamma_{out} \end{array} \right\} \tag{53}$$

and

$$\left.\begin{array}{rcl} \xi(s) - c\Delta\xi(s) + \nabla\pi(s) & = & 0 \quad \text{in } \Omega \\ -\delta t div\, \xi(s) & = & 0 \quad \text{in } \Omega \\ \xi(s) & = & \left\{ \begin{array}{ll} 0 & \text{on } \Gamma_d \\ \frac{1}{c}\nabla^2 F(\partial_\eta u(\phi^k))\partial_\eta u(s) & \text{on } \Gamma_s \end{array} \right. \\ c\partial_\eta \xi(s) & = & \pi(s)\eta \quad \text{on } \Gamma_{out}. \end{array} \right\} \tag{54}$$

From (46) and (48) with $(\xi(\rho), \pi(\rho))$ linearized according to (52) an approximation to the optimal step size is formed;

$$\rho^*_{app} = \frac{\int_{\Gamma_c} (\gamma\phi^k + c\partial_\eta \xi(\phi^k) - \pi(\phi^k)\eta) s \, d\Gamma_c}{\int_{\Gamma_c} (\gamma s + c\partial_\eta \xi(s) - \pi(s)) s \, d\Gamma_c}. \tag{55}$$

Every iteration of the gradient algorithm requires the solution of four quasi-Stokes problems: (50) and (53) for the evaluation of the gradient and two additional ones given by (51) and (54) for an approximation ρ^*_{app} to the optimal step length in the line search of problem (L). We note that in the case that F is quadratic (52) is exact and hence ρ^*_{app} gives the optimal step length for (L).

For the cost in (9) the elements of the Hessian must be interpreted as directional derivatives. Recalling that $\eta = (0, -1, 0)^t$, we obtain for the cost in (9)

$$\nabla F(\partial_\eta u) = \begin{pmatrix} -\frac{\partial u_1}{\partial x_2} + \left|\frac{\partial u_1}{\partial x_2}\right| \\ 0 \\ 0 \end{pmatrix}$$

The Hessian of F exists as directional derivative as long as $\frac{\partial u_1}{\partial x_2} \neq 0$. At $\frac{\partial u_1}{\partial x_2} = 0$ the functional F allows no second derivative. In practice we took

$$\nabla^2 F(\partial_\eta u)\partial_\eta w = \begin{pmatrix} \left[-1 + \operatorname{sign}\left(\frac{\partial u_1}{\partial x_2}\right)\right] \frac{\partial w_1}{\partial x_2} \\ 0 \\ 0 \end{pmatrix},$$

where

$$\operatorname{sign}(s) \ := \ \begin{cases} 1, & s \geq 0 \\ 0, & s < 0. \end{cases}$$

5 Numerical results

Here we present numerical results related to the approaches presented in the previous sections. Instantaneous control is applied to problem (10) involving cost functionals of tracking type (11) and of boundary observation type (9). As already mentioned the goal of the optimization is the reduction of the recirculation bubble behind the step and thus of the re-attachment length of the two-dimensional laminar Navier-Stokes flow at Reynolds numbers up to Re= 400. We investigate parameters determining the problem formulation as well as the step size in the gradient algorithm. For the discretization of the quasi-Stokes problems the Taylor-Hood finite element is used. Numerical solutions of various problems are performed using an extension of the Navier-Stokes solver developed by Bänsch in [2]. The control strategies applied here are based on first-order semi-implicit time discretization (explicit Euler for the nonlinear term, implicit Euler for the viscous term).

The computational domain is the backward-facing-step shown in Fig. 1. The inflow boundary is located at a distance of two step heights, i.e. $2h$ before the step, and an expansion ratio of 2 is used. The outflow boundary is located at a distance of $8h$ behind the step. The Reynolds number is based on the step height h and the bulk velocity U at the inlet. The boundary conditions are no-slip at the top and the bottom walls and *do-nothing* at the outflow boundary. For the spatial discretization the Taylor-Hood finite element is used on a grid containing 1152 triangles, 633 pressure and 2417 velocity nodes.

In all figures presented the label *Cost* refers to the evolution of the cost functional J, *Control Cost* refers to the evolution of the square of the L^2-norm of the control input taken over the control domain $\Omega_c = \Omega$ in the case of distributed control or Γ_c in the case of boundary control and, *Difference to Stokes Flow* refers to the evolution of the square of the L^2-norm in the whole of Ω of the difference between the controlled flow and the Stokes flow.

5.1 Distributed control (volume observations and volume control)

In this Section the numerical results for distributed control in the case of volume oberservations are presented. Although distributed control is not practical from the application point of view it serves as a first validation of the suboptimal control strategies.

Unless otherwise specified $\gamma = 1.e-2$ and $\Omega_s = [4,6] \times [-1,0]$. Moreover no control is applied in the time interval $[0,2)$. At $t=2$ control with fixed step size in the gradient algorithm is invoked and is applied up to $t=20$. From that moment on the gradient algorithm is used with optimal descent parameter ρ^* as explained in Section 4.

The cost function to be minimized at each time step in this case is given by

$$J(g) = \frac{1}{2}\int_{\Omega_s} |u - u_{st}|^2\, dx + \frac{\gamma}{2}\int_{\Omega} g^2\, dx,$$

where the control g is a volume force added to the right-hand-side of the state equations of the instantaneous control problem (compare (39)).

The costs for Re$=100, 200$ and 300 are presented in Fig. 2(a). Control is invoked at $t=2$. Up to $t=20$ at every time instance one gradient step is performed with descent parameter $\rho \approx \frac{\rho^*}{30}$. Starting at $t=20$, up to $t=50$ one gradient step using the optimal descent parameter ρ^* is performed at each time-level. As can be observed this is accomplished with nearly zero cost. At $t=50$ control is switched off and the flow evolves to the uncontrolled Navier-Stokes flow at the corresponding Reynolds number. In Figs. 2(b) and (c) the evolution of the square of the L^2-norm of the control cost $||g||^2_\Omega$ and the square of the L^2-difference $||u-\bar{u}||^2_\Omega$ of the flow to the Stokes flow in the whole domain are presented. As is expected the control cost and the difference to the Stokes flow become larger as the Reynolds number increases.

Fig. 3 shows the uncontrolled Navier-Stokes flow at Re$=300$ (a) together with the control target Stokes flow (b), the control force g (c) and the controlled flow at $t=50$ (d). As one can see the controlled flow fits well to the Stokes flow in the observation volume Ω_s. The numerical results for Re=100 and 200 are similar and are therefore omitted.

Next we investigate the influence of the number of gradient iterations on the control output. For this purpose we compare the numerical results for one gradient iteration per time step to those for three iterations. In Figs. 4 (a), (b) and (c) the evolutions of the cost, the control cost and the L^2-difference to the Stokes flow are presented. It can be seen that three gradient steps yield smaller costs while the controls are slightly more expensive.

5.2 Boundary control

In this Section we present numerical results for boundary controls in the cases of volume and boundary observations.

5.2.1 Volume observations

In this section we present the numerical results for the case of the reconstruction of the Stokes flow in a given observation volume $\Omega_s \subset \Omega$ behind the step of the flow domain. The functional to be minimized at each time instance is related to the functional J_1 in (11) and is given by

$$J(\phi) = \frac{1}{2}\int_{\Omega_s} |u - u_{st}|^2\, dx + \frac{\gamma}{2}\int_{\Gamma_c} \phi^2\, d\Gamma_c,$$

where ϕ denotes the boundary control applied at the upper part of the back wall $[2,2] \times [-0.5,0] \subset \Gamma_c$. In all numerical computations presented we set Re$=400$. Control is invoked at $t=2$ up to $t=20$ with descent parameter $\rho = 1$ in the gradient step. At $t = 20$ up to $t = 100$ the optimal descent parameter ρ^* is used to compute the controls. One gradient step is performed per time instance.

Now the influence of the varying penalty parameter γ on the controls is investigated. In Tab. 1 the optimal descent parameters corresponding to the penalty parameters γ are shown. Note that the optimal descent parameters remain nearly constant over the whole time integration interval since the control problem at each time instance is of tracking-type with linear constraints. Fig. 5(a) shows the evolution of the costs. For

γ	1.e0	1.e-1	1.e-2	1.e-3
ρ^*	0.82	3.13	4.35	4.53

Table 1: Optimal descent parameter ρ^* with the corresponding penalty parameter γ at Re= 400

$\gamma = 1$ one observes increasing costs for $t \in [20, 30]$. This is due to the suboptimal character of the approach. Decreasing γ yields decreased costs at time instances where the controls are stationary. The oscillations in the costs for small γ are due to the instantaneous character of the feedback control mechanism. As Fig. 6 shows, these effects can be damped by performing further gradient steps in the instantaneous control problems. One also observes that the robustness of the feedback controller increases with the number of gradient steps.

In the evolution of the control costs in Fig. 5(b) one also observes oscillations of the control after the inset of the use of the optimal descent parameter ρ^*. However, the oscillations disappear with time and the control costs converge to steady states. Thus, the feedback control mechanism is stable. The same holds true for the evolution of the L^2-difference of the flow to the Stokes flow in Fig 5(c). The feedback controller presented here yields a significant reduction of the costs of all targets under consideration. The controlled flows for different penalty parameters are shown in Fig.7

5.2.2 Boundary observations

In this section we present numerical investigations on the influence of sensor area Γ_s on the feedback control mechanism. The functional to be minimized at each time instance is related to the functional J in (9) and is given by

$$J(\phi) = \frac{1}{2}\int_{\Gamma_s} \frac{\partial u_1}{\partial x_2}\left(\frac{\partial u_1}{\partial x_2} - \left|\frac{\partial u_1}{\partial x_2}\right|\right) d\Gamma_s + \frac{\gamma}{2}\int_{\Gamma_c} \phi^2 \, d\Gamma_c,$$

where again ϕ denotes the boundary control applied at the upper part of the back wall Γ_c and u_1 denotes the stream-wise velocity. Consequently, the first part in the cost functional vanishes when there is no recirculation region at Γ_s.

In Fig. 8 the flows corresponding to different sizes of Γ_s are shown. It can be observed that the larger the distance between the control boundary Γ_c and the sensor area Γ_s, the more the control mechanism becomes periodic. This is due to the fact that without control the flow evolves to the uncontrolled Navier-Stokes flow and the time span lapsing untill the evolving flow affects the sensor area is larger for larger distances between Γ_c and Γ_s. This can also be observed for the evolution of the costs in Fig. 9(a) and the costs of the boundary control in Fig. 9(b). Of course, the controlled flow also depends on the size of Γ_s but experiments show that it plays a less important role.

Remark 5.1 *In order to validate further the numerical approaches presented in this research the control strategies presented have also been applied to the Navier-Stokes flow with random forcing acting on the flow in the observation volume Ω_s. In this case, the uncontrolled flow shows a chaotic caracteristics. In all test* *cases the constructed feedback laws led to succesful results since they yielded remarkable reductions of the cost and the flows converge to a statistically steady state.*

6 Conclusion and discussion

In the present paper we have addressed a typical control problem in fluid dynamics, namely, the reduction of the re-attachment length of a backward facing step flow. To capture this goal for laminar 2D flows we have implemented several feedback procedures in the numerical part of the paper. In the theoretical part we provide a general frame to obtain feedback laws for the time dependent Navier-Stokes equations using Lagrangian techniques applied to instantaneous control problems.

Two types of controls have been investigated: distributed and boundary controls. Although distributed control by body forces based on volume observations in prescribed observation volumes is impractical from the application point of view it served as a first validation and as comparison to boundary control strategies. For boundary control, the control is the boundary velocity at the upper part of the back wall. This control is more practical and can be implemented in real situations, especially when based solely on wall velocity gradients of the flow, see (39).

Several case studies for both types of controls were completed to investigate the sensitivity of the feedback laws w.r.t. the parameters involved: the dependence on the Reynolds number , the number of gradient steps and the effect of the descent parameter on the gradient algorithm for distributed control, and for boundary control the influence of control cost penalization , the position of the sensor area for boundary observation and as for distributed control, the dependence on the number of gradient steps as well as the effect of the descent parameter on the performance of the gradient algorithm. In nearly all cases a significant reduction of the cost was obtained. Especially for boundary control the use of the near to optimal descent parameter (55) in the gradient algorithm gave excellent results.

A semi-implicit method (explicit Euler for the nonlinearity, implicit Euler for the viscous term) has been used for the numerical computations since, for boundary control based on a fully implicit method the adjoint equations contain the velocity of the flow in the whole domain of computation as well as boundary velocity gradients (compare (37)). That is, full knowledge of the flow field would be required for the implementation of the feedback law when using a fully implicit time integration scheme, even if the closed-loop system is based solely on boundary observations. The use of semi-implicit time integration circumvents this problem.

The procedure developed in this paper can be practically realized as suboptimal feedback mechanism. Already one gradient step at each time instance led to a significant reduction of the cost. This was especially welldemonstrated in the case of boundary controls based on boundary observations provided the distance of sensor area and control boundary, i.e. time delay in the system, is not too large.

Acknowledgments

The first author acknowledges the support from Korea Science and Engineering Foundation under Contract No. 96-0200-01-01-2. The second and third authors acknowledge the support of the University Research Grant 8 (UF8) at the Technical University of Berlin, Germany.

References

[1] **Abergel, F.; Temam, R.** *On some Control Problems in Fluid Mechanics* Theoret. Comput. Fluid Dynamics 1 (303-325), 1990.

[2] **Bänsch, E.** *An adaptive Finite-Element-Strategy for the three-dimensional time-dependent Navier-Stokes-Equations* J. Comp. Math. 36 (3-28), 1991.

[3] **Choi, H; Temam, R.; Moin, P.; Kim, J.** *Feedback control for unsteady flow and its application to the stochastic Burgers equation* J. Fluid Mech. 253 (509 pp.), 1993.

[4] **Heywood, J.G.; Rannacher, R.; Turek, S.** *Artificial Boundaries and Flux and Pressure Conditions for the Incompressible Navier-Stokes Equations* Preprint 94 - 06, SFB 359, Universität Heidelberg, 1994.

[5] **Hinze, M.; Koster, F.** Preprint in preparation, Technische Universität Berlin, 1997.

7 Figures

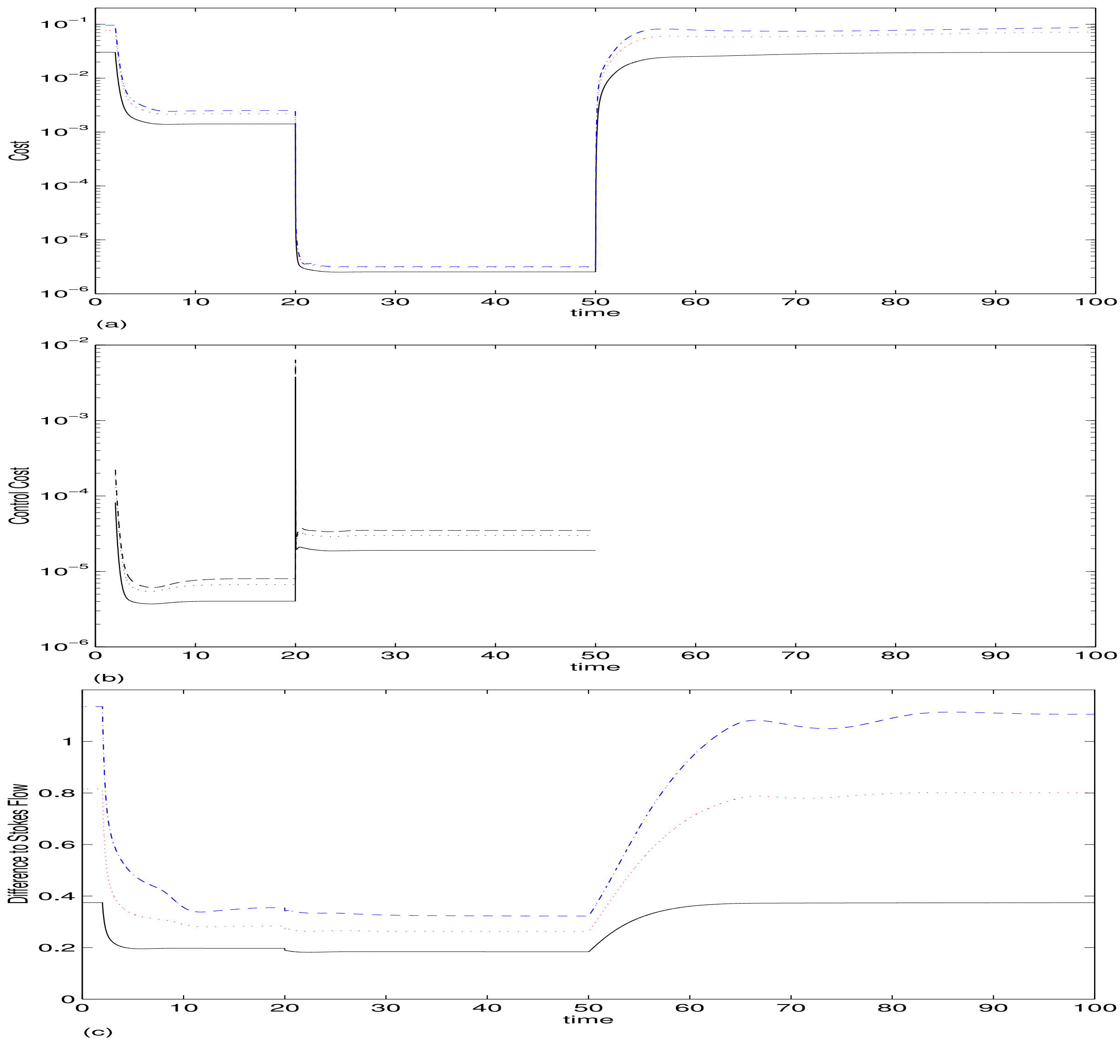

Figure 2: Distributed control at Re=100(solid), 200(dotted), 300(dashed): (a) Cost; (b) Control Cost; (c) Difference to Stokes Flow

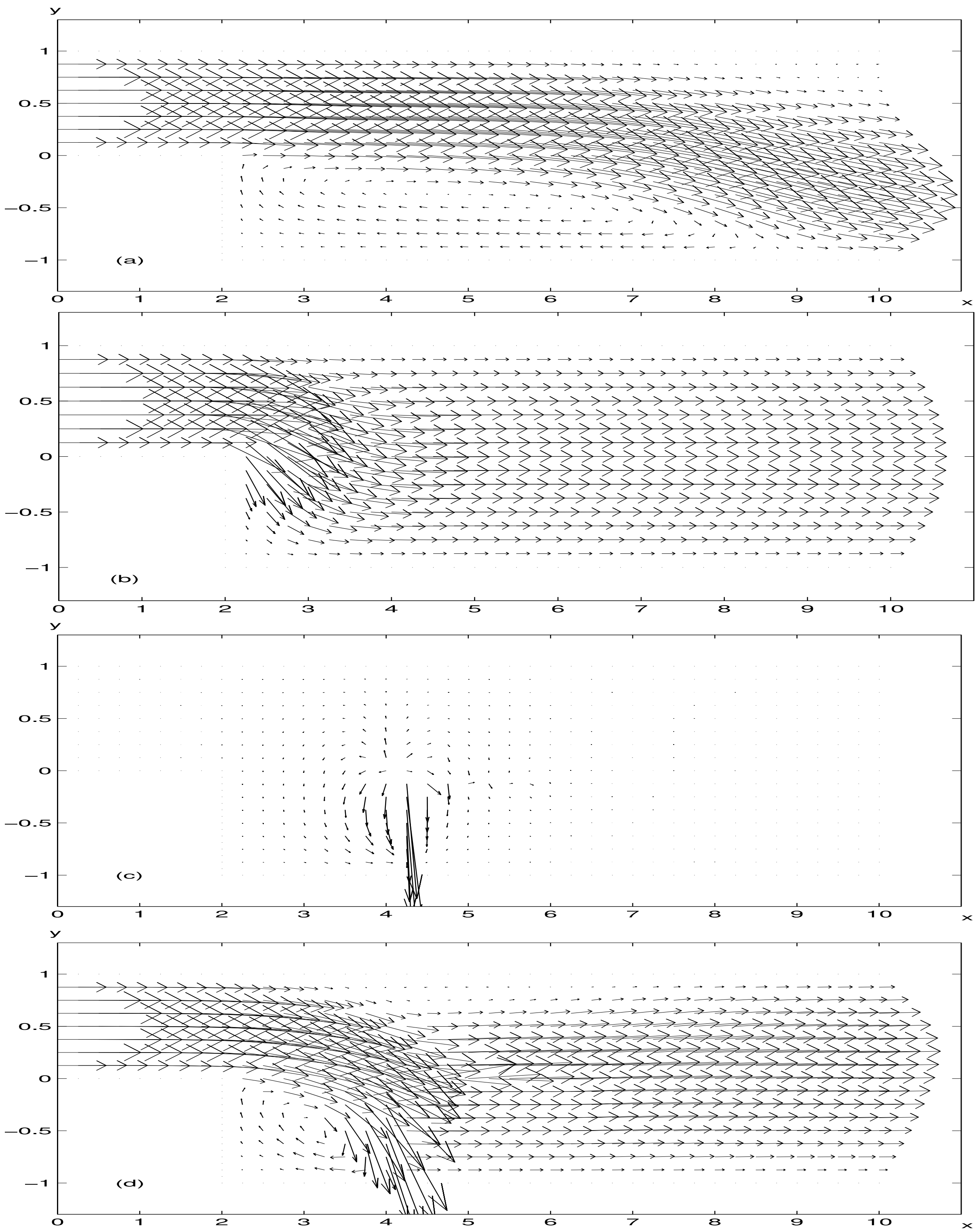

Figure 3: Distributed control at Re=300: (a) Navier-Stokes flow; (b) Stokes flow; (c) Control force at $t = 50$; (d) Controlled flow at $t = 50$

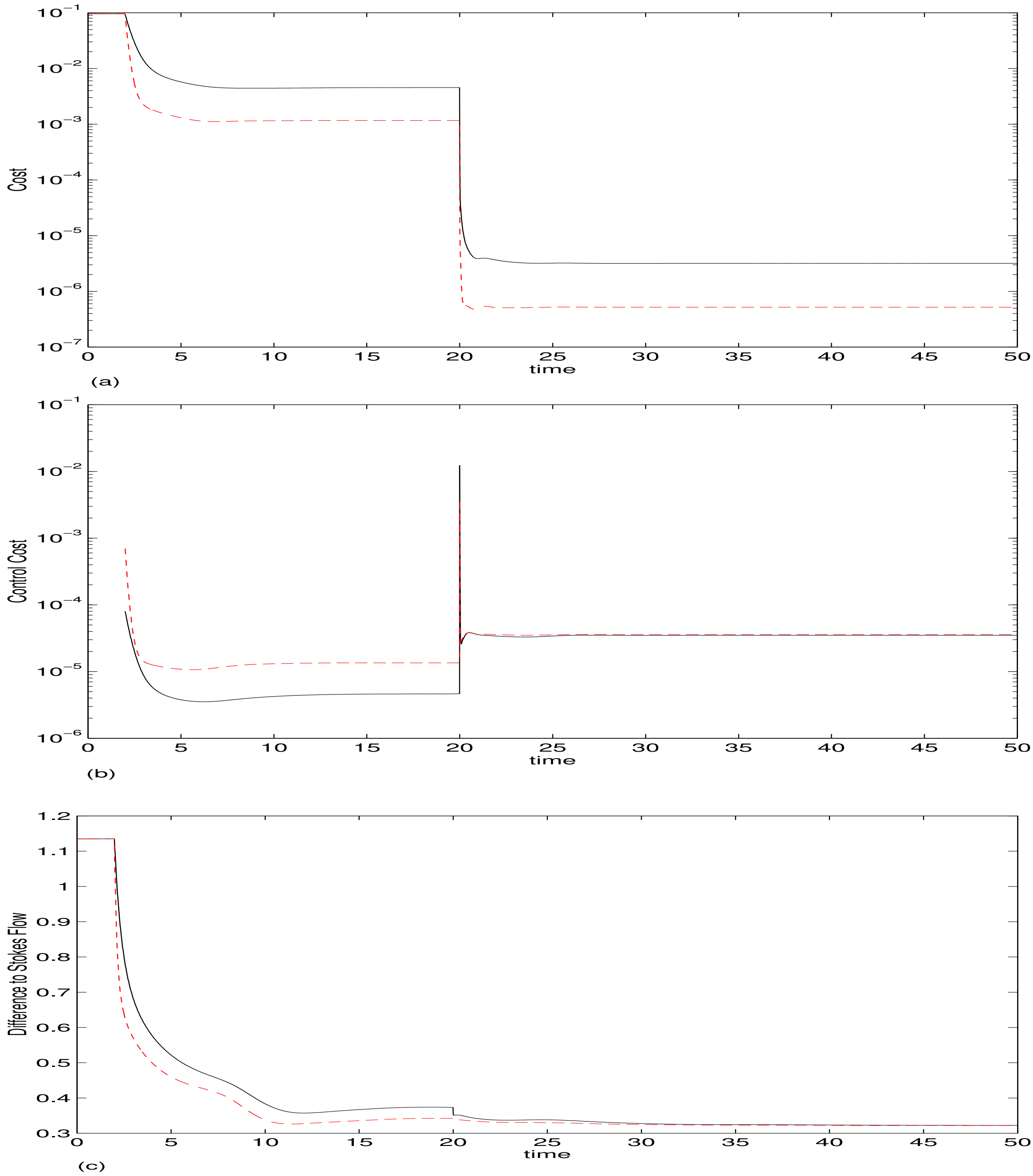

Figure 4: Distributed control at Re=300 : 1 Gradient Step (solid); 3 Gradient Steps (dashed). (a) Cost; (b) Control Cost; (c) Difference to Stokes Flow

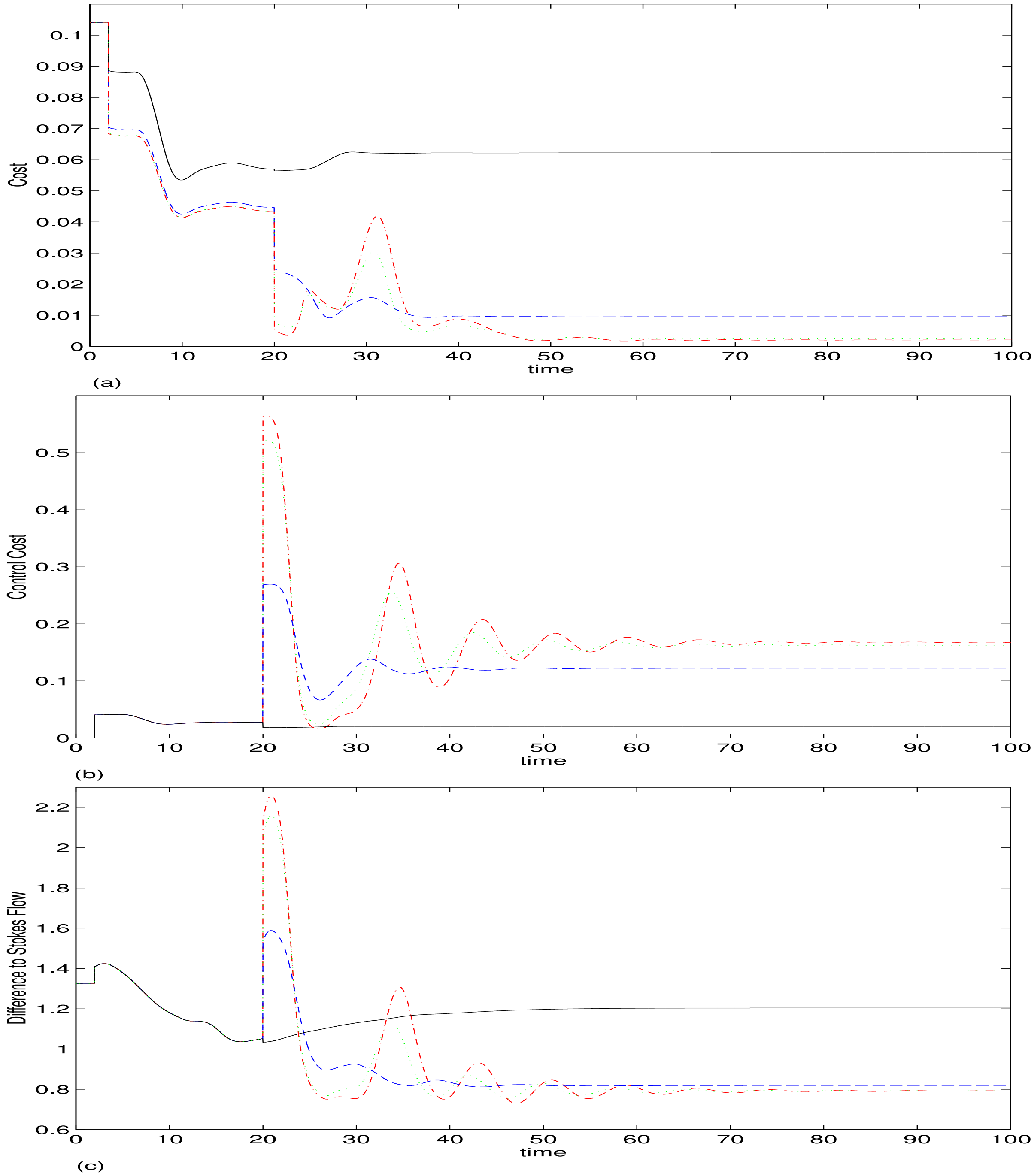

Figure 5: Boundary control at Re=400: γ =1(solid), 1.e-1(dashed), 1.e-2(dotted), 1.e-3(dash-dotted). (a) Cost; (b) Control Cost; (c) Difference to Stokes Flow

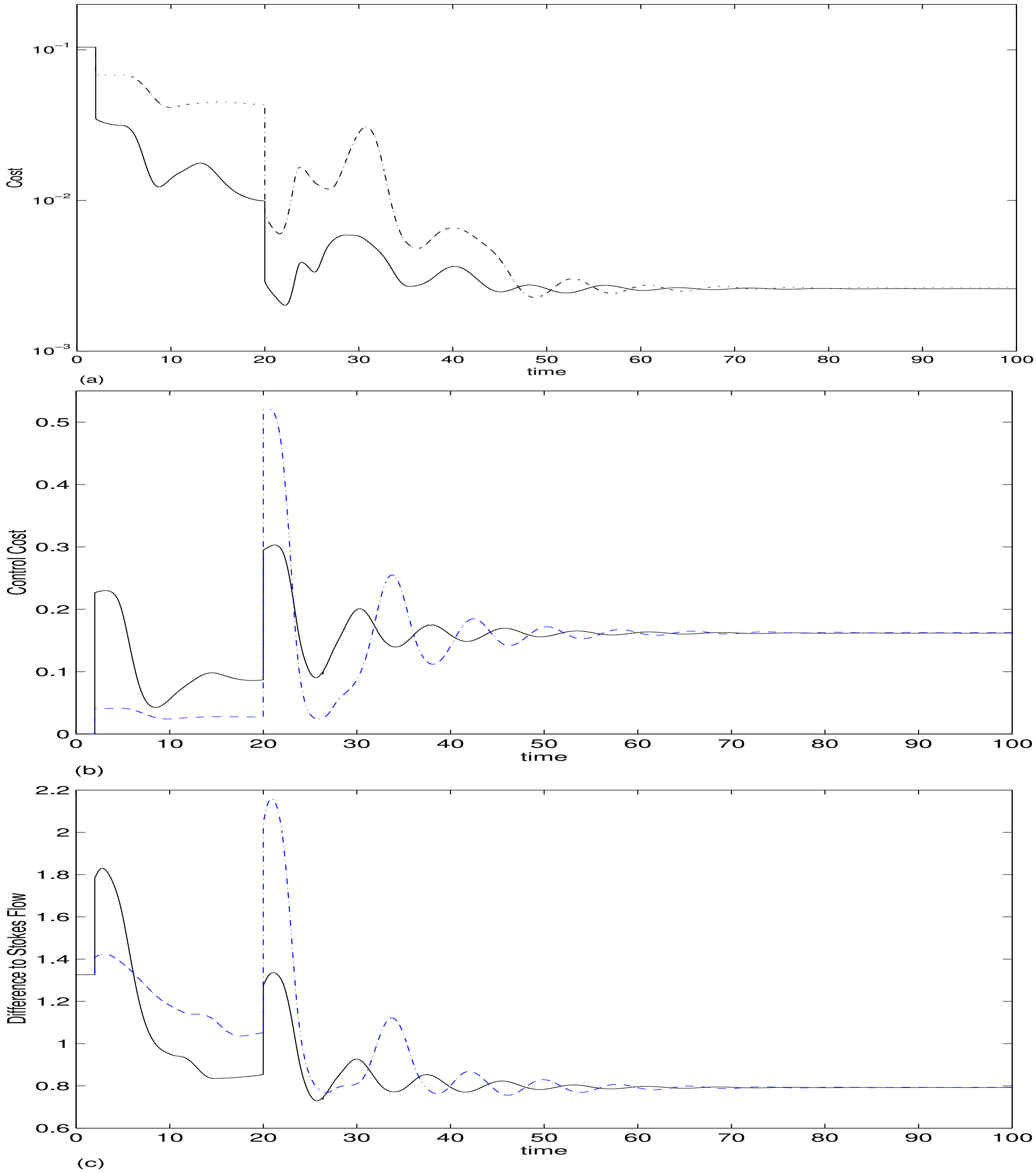

Figure 6: Boundary control at Re=400, $\gamma = 1.e - 2$: 3 gradient steps(solid), 1 gradient step(dash-dotted). (a) Cost; (b) Control Cost; (c) Difference to Stokes Flow

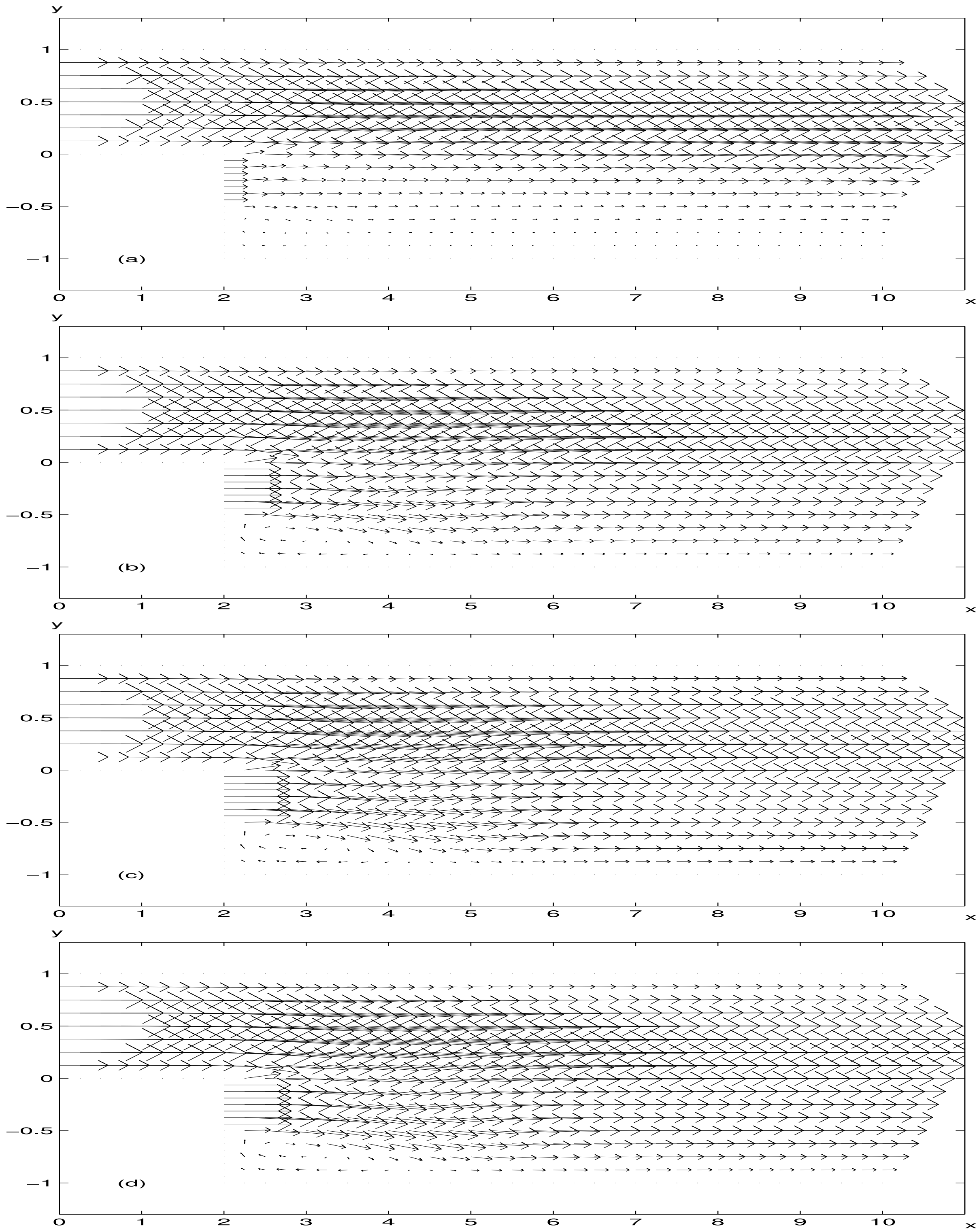

Figure 7: Boundary control at Re= 400: Controlled flows at $t = 100$. (a) γ =1; (b) γ =1.e-1; (c) γ =1.e-2; (d) γ =1.e-3

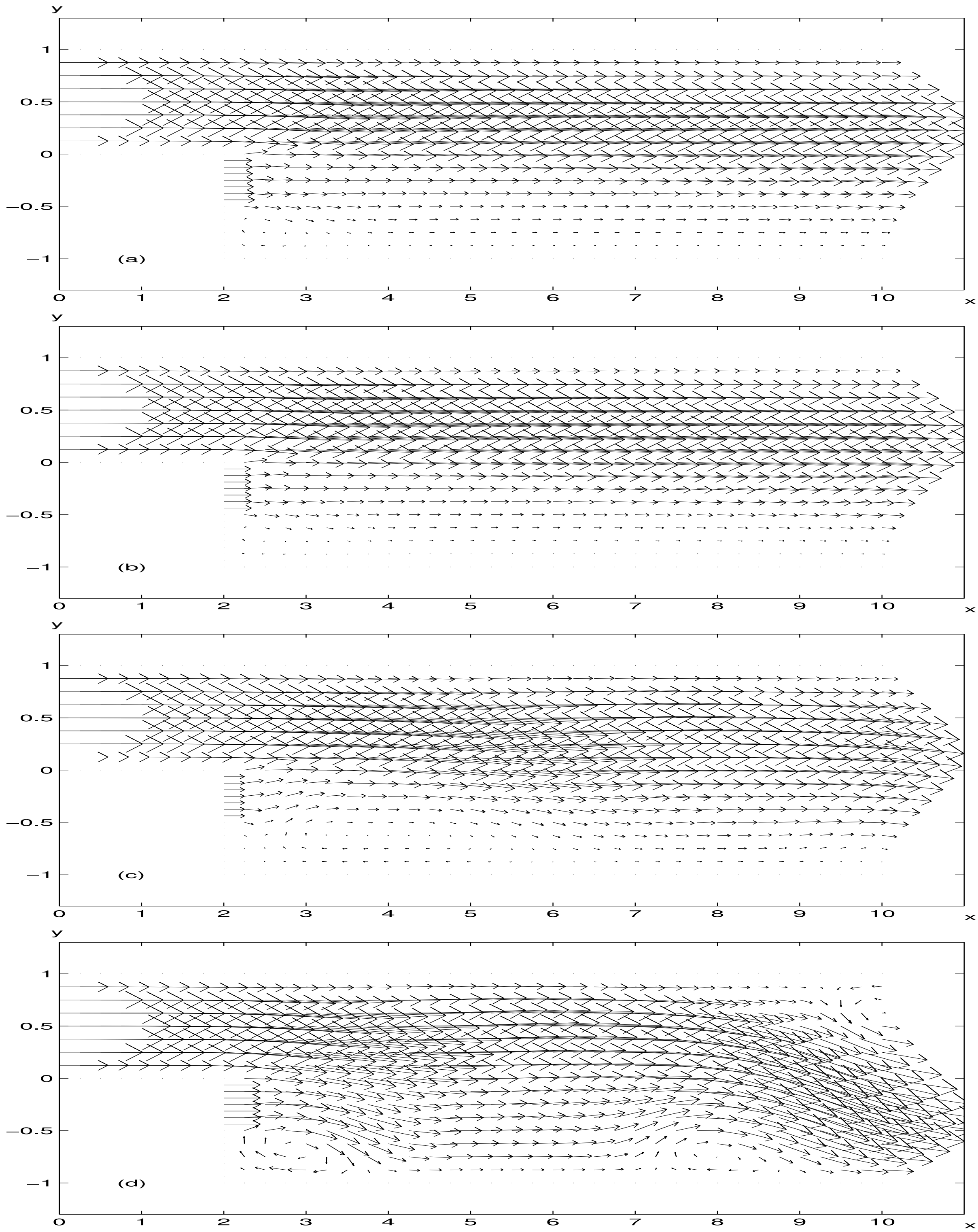

Figure 8: Boundary control based on boundary observation at Re= 300: Controlled flows for (a) $\Gamma_s = [2, 9]$; (b) $\Gamma_s = [3, 9]$; (c) $\Gamma_s = [4, 9]$; (d) $\Gamma_s = [5, 9]$

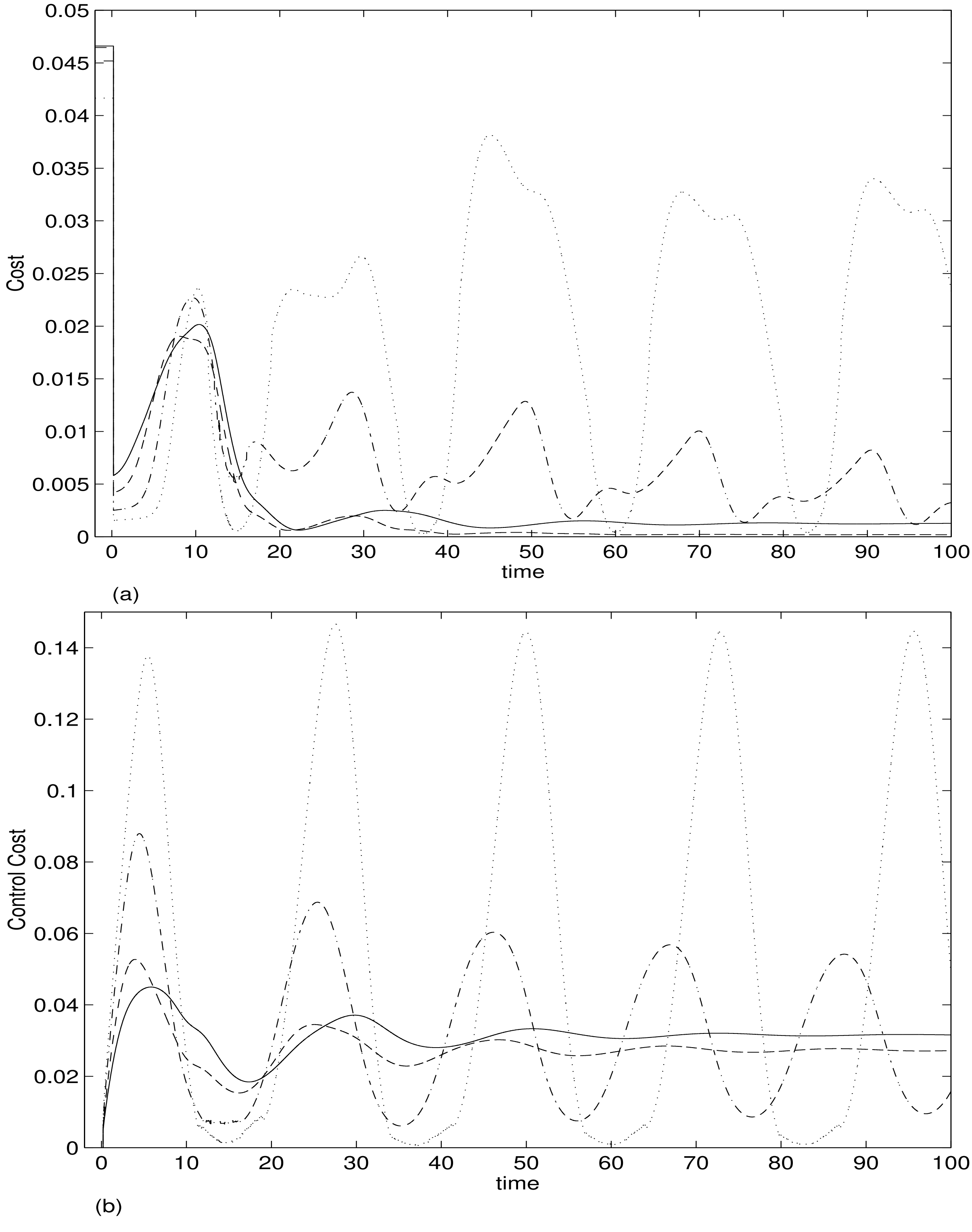

Figure 9: Boundary observation at Re=300: $\Gamma_s = [2,9]$(solid), $[3,9]$(dashed), $[4,9]$(dash-dotted), $[5,9]$(dotted). (a) Cost; (b) Control Cost